Contributions of molecular binding events and cellular compliance to the modulation of leukocyte adhesion

Ewa P. Wojcikiewicz, Xiaohui Zhang, Aileen Chen and Vincent T. Moy*

Department of Physiology and Biophysics, University of Miami School of Medicine, Miami, FL 33136, USA

*Author for correspondence (e-mail: vmoy@miami.edu)

Accepted 7 March 2003
Journal of Cell Science 116, 2531-2539 © 2003 The Company of Biologists Ltd
doi:10.1242/jcs.00465

Summary

The interaction of leukocyte function-associated antigen-1 (LFA-1) and intercellular adhesion molecule-1 (ICAM-1) is central to the regulation of adhesion in leukocytes. In this report, we investigated the mechanisms by which phorbol myristate acetate (PMA) promotes LFA-1-dependent cell adhesion. The adhesion of PMA-stimulated cells to immobilized ICAM-1 was quantified in direct force measurements acquired by atomic force microscopy (AFM). Enhanced adhesion of PMA-stimulated cells to immobilized ICAM-1 stemmed from an increase in the number of LFA-1–ICAM-1 complexes formed between the two apposing surfaces on contact, rather than by affinity modulation of LFA-1. Single molecule force measurements revealed that the force spectrum of the LFA-1–ICAM-1 complex formed by PMA-stimulated cells is identical to the force spectrum of the complex formed by resting cells. Thus, PMA stimulation does not modify the mechanical strength of the individual LFA-1–ICAM-1 interaction. Instead, the enhanced cell adhesion of PMA-stimulated cells appears to be a complex process that correlates with changes in the mechanical properties of the cell. We estimate that changes in the elasticity of the cell gave rise to a more than 10-fold increase in cell adhesion.

Key words: Cell adhesion, Cell compliance, Integrins, Leukocyte, AFM, Single molecule measurements

Introduction

The regulation of leukocyte adhesion to target cells is crucial for the body's immune response. Leukocyte adhesion is largely mediated by surface receptors, including the integrins and members of the immunoglobulin superfamily (Springer, 1990). Integrins are αβ heterodimeric glycoproteins derived from the noncovalent association of one of 18 α chains and one of 8 β chains (Hynes, 1992). In leukocytes, α_L combines with β_2 to form LFA-1, the major leukocyte integrin (Sanchez-Madrid et al., 1983). LFA-1 facilitates leukocyte adhesion by binding to its ligands, which include intercellular adhesion molecule-1 (ICAM-1) found on the target cell (Marlin and Springer, 1987).

An important attribute of integrins is their ability to modulate the adhesive states of cells (Dustin and Springer, 1991; Diamond and Springer, 1994). In resting lymphocytes, LFA-1 is expressed in an inactive, nonadherent state; LFA-1 in this state binds ICAM-1 with low affinity. Upon engagement by an antigen presenting cell (APC), the T lymphocyte expresses an activated form of LFA-1 and becomes adherent to the APC. The interaction between a T lymphocyte and an APC is transient, with the adherent state lasting long enough for the T lymphocyte to become activated before it detaches from the APC.

Proposed mechanisms for the regulation of integrin-mediated leukocyte adhesion include receptor affinity modulation and clustering of integrins (avidity modulation) (Lollo et al., 1993; Woska et al., 1996; Lupher et al., 2001; Stewart and Hogg, 1996; van Kooyk and Figdor, 2000). Affinity modulation of LFA-1 is initiated by the engagement of surface receptors and involves a conformational change in the I domain of the α chain, leading to an opening of the ICAM-1-binding site (Shimaoka et al., 2002). The mechanism for affinity modulation in activated cells involves an inside-out signal that acts on the cytoplasmic domain of the β chain of LFA-1 (Hughes et al., 1996). The intramolecular transduction signal crosses the α chain via the βI domain/β-propeller junction, which then activates the I domain (Lu et al., 2001). The requirements for an inside-out signal for the induction of high-affinity LFA-1 can be circumvented by a high concentration of extracellular Mg^{2+} and by certain antibodies directed against the β chain (Ganpule et al., 1997; Huth et al., 2000). Recent studies suggest that extracellular Mg^{2+} activates LFA-1 by binding to the βI domain, which subsequently induced a conformational change in the I domain via the β-propeller (Lu et al., 2001).

Although the term avidity is frequently used in the context of cell adhesion, it remains poorly defined. Generally, avidity modulation refers to the redistribution or clustering of receptors that results in augmented cell adhesion. This loose definition of avidity may include several underlying mechanisms such as polarization of receptors to the zone of cell-cell contact, clustering of receptors to form focal adhesion sites and dimerization of receptors. A redistribution of receptors augments adhesion by increasing the receptor density at the site of cell-cell contact. A clustering of receptors allows for a more even distribution of the applied force and thus permits the clustered receptors to support greater forces than when the receptors are dispersed. In the latter case, there is an increased likelihood that an applied force will rupture the adhesion complex sequentially. The dimerization of receptors may result in the formation of a dimeric complex that functions as a cooperative unit that ruptures simultaneously. Although

the relative contribution of these underlying mechanisms to adhesion still needs to be resolved, it is well-documented that the initial event in avidity modulation in leukocyte adhesion is the release of LFA-1 from cytoskeletal constraints (Stewart et al., 1998). This is achieved following engagement of the antigen receptor for T lymphocytes and various surface receptors of migrating leukocytes. Recent studies using interference-reflection microscopy (IRM) have shown this mobilization of LFA-1 on T lymphocytes in contact with APCs. Once released from the cytoskeleton, the receptor molecules form ring-like structures termed supramolecular activation clusters (SMACs). The SMACs consist of antigen receptors localized at the center of cell-cell contact and LFA-1–ICAM-1 complexes in the periphery (Monks et al., 1998; Grakoui et al., 1999). These studies suggest that cytoskeletal remodeling plays an important role in T lymphocyte adhesion.

The mobilization of LFA-1, leading to enhanced adhesion, can be induced by pharmaceutical agents such as phorbol myristate acetate (PMA) (Rothlein and Springer, 1986). PMA is a potent activator of protein kinase C (PKC) and exerts its effects on intracellular pathways, bypassing the requirement for surface receptor engagement (Berry and Nishizuka, 1990). The activation of PKC leads to an increase in intracellular Ca^{2+} concentrations, Ins(1,4,5)P_3 kinase activity and phosphorylation of MacMARCKS and L-plastin (van Kooyk and Figdor, 2000; Zhou and Li, 2000; Jones et al., 1998). Elevated levels of intracellular Ca^{2+} subsequently activate the Ca^{2+}-dependent protease calpain, which releases LFA-1 from the cytoskeleton (Stewart et al., 1998). PMA also acts indirectly on the activity of cytohesin-1, which induces cytoskeletal reorganization and subsequently promotes cell spreading (Kolanus et al., 1996).

The current study employed the atomic force microscope (AFM) to elucidate how PMA stimulation of leukocytes enhances cell adhesion. AFM measurements of cell adhesion and cell compliance were carried out using the 3A9 cell line, a murine T-cell hybridoma that expresses the LFA-1 integrin but no other receptor for ICAM-1 (Lollo et al., 1993). LFA-1 of 3A9 cells is constitutively inactive but can be activated to a high-avidity state by PMA. Our research focused on the initial interaction between the 3A9 cells and immobilized ICAM-1. The enhanced adhesion of 3A9 cells following the addition of PMA was immediate and stemmed from a change in the mechanical properties of the cell rather than a change in the bond strength of the individual LFA-1–ICAM-1 complex.

Materials and Methods

Cells and reagents

The 3A9 cell line was maintained in continuous culture in RPMI 1640 medium supplemented with 10% heat-inactivated fetal calf serum (Irvine Scientific, Santa Ana, CA), penicillin (50 U/ml, Gibco BRL, Grand Island, NY) and streptomycin (50 μg/ml, Gibco BRL), and the cells were expanded on a 3-day cycle (Kuhlman et al., 1991).

ICAM-1/Fc chimera consisted of all five extracellular domains of murine ICAM-1 (Gln 28-Asn 485) and the Fc fragment of human IgG_1 and was purchased from R & D Systems, Inc. (Minneapolis, MN). The ability of this protein to bind LFA-1 was confirmed using ELISA and adhesion assays. From these experiments, we were able to conclude that the LFA-1-binding epitope D1 of ICAM-1 is available for binding. Antibodies against LFA-1 (i.e. M17/4.2 and FD441.8) and against ICAM-1 (i.e. BE29G1) were purified from culture supernatant by protein G affinity chromatography (Sanchez-Madrid et al., 1983; Kuhlman et al., 1991). Stock solutions of PMA (10,000×) (Sigma, St. Louis, MO) were prepared at 1 mM in DMSO.

Protein immobilization

25 μl of ICAM-1/Fc at 50 μg/ml in 0.1 M $NaHCO_3$ (pH 8.6) was adsorbed overnight at 4°C on the center of a 35 mm tissue culture dish (Falcon 353001, Becton Dickinson Labware, Franklin Lakes, NJ). Unbound ICAM-1/Fc was removed and bovine albumin (Sigma) at 100 μg/ml in PBS was used to block the exposed surface of the dish. A similar protocol was used to immobilize the anti-LFA-1 antibodies (i.e. FD441.8 and M17/4.2).

AFM measurements of adhesive forces

The AFM force measurements were performed on an apparatus designed to be operated in the force spectroscopy mode (Benoit et al., 2000; Heinz and Hoh, 1999; Willemsen et al., 2000). 3A9 cells were attached to the AFM cantilever by concanavalin A (conA)-mediated linkages (Zhang et al., 2002). To prepare the conA-functionalized cantilever, the cantilevers were soaked in acetone for 5 minutes, UV irradiated for 30 minutes and incubated in biotinamidocaproyl-labeled bovine serum albumin (biotin-BSA, 0.5 mg/ml in 100 mM $NaHCO_3$, pH 8.6; Sigma) overnight at 37°C. The cantilevers were then rinsed three times with phosphate-buffered saline (PBS, 10 mM PO_4^{3-}, 150 mM NaCl, pH 7.3) and incubated in streptavidin (0.5 mg/ml in PBS; Pierce; Rockford, IL) for 10 minutes at room temperature. Following the removal of unbound streptavidin, the cantilevers were incubated in biotinylated conA (0.2 mg/ml in PBS; Sigma) and then rinsed with PBS.

To attach the 3A9 cell to the cantilever, the end of the conA-functionalized cantilever was positioned above the center of a cell and carefully lowered onto the cell for approximately 1 second. When attached, the cell is positioned right behind the AFM tip of the cantilever as illustrated in Fig. 1. To obtain an estimate of the strength of the cell-cantilever linkage, we allowed the attached cell to interact with a substrate coated with conA for 1 minute. Upon retraction of the cantilever, separation (N>20) always occurred between the cell and the conA-coated surface. The average force needed to induce separation was greater than 2 nN. These measurements, thus, revealed that the linkages supporting cell attachment to the cantilever is greater than 2 nN and much larger than the detachment force required to separate the bound 3A9 cell from immobilized ICAM-1 (Zhang et al., 2002).

A piezoelectric translator was used to lower the cantilever/cell onto the sample. The interaction between the attached 3A9 cell and the sample was given by the deflection of the cantilever, which was measured by reflecting a laser beam off the cantilever into a position sensitive 2-segment photodiode detector. AFM cantilevers were purchased from TM Microscopes (Sunnyvale, CA). The largest triangular cantilever (320 μm long and 22 μm wide) from a set of five on the cantilever chip was used in our measurements. These cantilevers were calibrated by analysis of their thermally induced fluctuation to determine their spring constant (Hutter and Bechhoefer, 1993). The experimentally determined spring constants were consistent with the nominal value of 10 mN/m given by the manufacturer.

AFM force measurements of individual LFA-1–ICAM-1 complexes

Measurements of unitary LFA-1-ICAM-1-unbinding forces were obtained under conditions that minimized contact between the 3A9 cell and the sample. An adhesion frequency of <30% in the force measurements ensured that there is a >85% probability that the adhesion event is mediated by a single LFA-1–ICAM-1 bond (Zhang et al., 2002).

Data were corrected for hydrodynamic drag. Our determination of the hydrodynamic force was based on the method used by Tees et al. and Evans et al. (Tees et al., 2001; Evans et al., 2001). We allowed the cantilever to undergo free movement at different speeds, and the hydrodynamic force for each speed was measured. These data suggest that the hydrodynamic force acts in the opposite direction of cantilever movement, and its magnitude is proportional to the cantilever movement speeds. In this report the data obtained with cantilever retraction speeds higher than 1 μm/s were corrected by adding the hydrodynamic force.

To determine the damping coefficient, we plotted the hydrodynamic force versus speed of cantilever movement. The damping coefficient is the slope of the linear fit and is about 2 pN•s/μm (Zhang et al., 2002).

AFM measurements of cell elasticity

In this report, the AFM served a dual purpose: first as a pulling device to detach adherent cells (described above), and secondly, as a microindenter that probes the mechanical properties of the cell. In the cell elasticity measurements, the bare AFM tip is lowered onto the cell surface at a set rate, typically 2 μm/second. After contact, the AFM tip exerts a force against the cell that is proportional to the deflection of the cantilever. The deflection of the cantilever was recorded as a function of the piezoelectric translator position during the approach and withdrawal of the AFM tip. The force-indentation curves of the cells were derived from these records using the surface of the tissue culture dish to calibrate the deflection of the cantilever. Estimates of Young's modulus were made on the assumptions that the cell is an isotropic elastic solid and the AFM tip is a rigid cone (Wu et al., 1998; Hoh and Schoenenberger, 1994; Radmacher et al., 1996). According to this model, initially proposed by Hertz, the force (F)-indentation (α) relation is a function of Young's modulus of the cell, K, and the angle formed by the indenter and the plane of the surface, τ, as follows:

$$F = \frac{K}{2(1-\nu^2)} \frac{4}{\pi \tan\theta} \alpha^2. \quad (1)$$

Young's modulus was obtained by least square analysis of the force-indentation curve using routines in the Igor Pro (WaveMetrics, Inc., Lake Oswego, OR) software package. The indenter angle, τ, and Poisson ratio, ν, were assumed to be 55° and 0.5, respectively.

Measurements of cell adhesion and elasticity were carried out at 25°C in fresh tissue culture medium supplemented with 10 mM HEPES buffer. Cells were stimulated by 5 mM $MgCl_2$ plus 1 mM EGTA or 100 nM PMA. The activation of 3A9 by Mg^{2+} was immediate. 3A9 cells were exposed to PMA for ~5 minutes at 37°C prior to the start of the experiments. All experiments involved making contact with the same cell up to 50 times. There was no dependence on previous contacts observed in either the elasticity or adhesion AFM studies.

Results

AFM measurements of integrin-mediated cell adhesion

Direct force measurements of the adhesive interaction between a 3A9 cell and immobilized ICAM-1 were carried out by AFM. As described in Materials and Methods, the 3A9 cell was coupled to the end of an AFM cantilever, and ICAM-1/Fc was immobilized on the surface of a tissue culture dish. Fig. 1 illustrates the steps in the acquisition of the AFM force measurements. During the approach trace, the cell was lowered onto the surface of the ICAM-1. Following contact, cell-substrate adhesion was detected during the contraction of the piezoelectric translator, which retracts the cantilever, pulling the cell off from the substrate. The tension between the cell and immobilized ICAM-1 was determined from the deflection of the cantilever. Fig. 2 presents a series of measurements using this protocol.

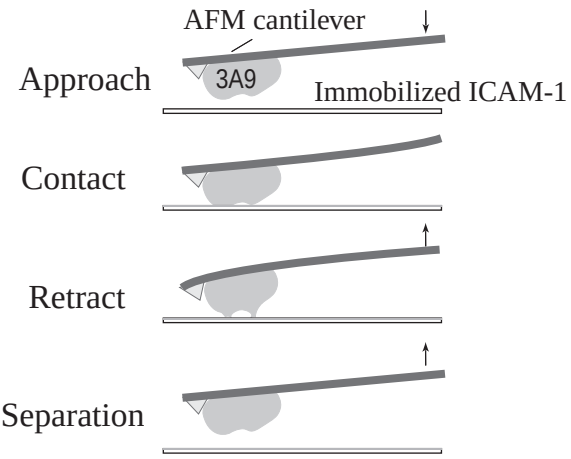

Fig. 1. Schematics of AFM force measurements. The principal events of cell-substrate interaction during an AFM force versus displacement measurement are approach of the 3A9 cell onto a surface coated with ICAM-1, contact between cell and substrate, retraction of the 3A9 cell and separation of the cell from the substrate. Arrows indicate the direction of cantilever movement.

AFM measurements of the detachment of the cell from the ICAM-1-coated dishes revealed a complex process. The measurements showed that the cells detached through a series of jumps (as indicated by arrows in Fig. 2) in force before final separation. Each of the force jumps (breakage force) in the retraction trace were interpreted as the breakage of one or more LFA-1–ICAM-1 bonds of >50 pN (Zhang et al., 2002). The number of LFA-1–ICAM-1 complexes depended on various factors, including the compression force that pressed the cell against the substrate and the duration of cell-substrate contact. During the retraction of the cantilever, the cell is stretched with elongations of several microns, possibly stemming from tether formations (Benoit, 2002).

In the current study, we investigated the mechanisms of enhanced cell adhesion to immobilized ICAM-1 following cell activation. Enhanced cell adhesion to immobilized ICAM-1 was induced by either 5 mM $MgCl_2$/1 mM EGTA or 100 nM PMA. Fig. 2 presents a series of measurements carried out under identical conditions (i.e. 200 pN compression force, 5 seconds contact and 2 μm/second retraction speed) with resting (first trace), Mg^{2+}-treated (second trace) and PMA-stimulated (third trace) cells. Both Mg^{2+}-treated and PMA-stimulated cells adhered more to immobilized ICAM-1 than resting cells, as was evident by the larger maximum force required to dislodge the cell (detachment force, f_{de}). Moreover, the number of rupture events is significantly greater for PMA-stimulated cells than is the case of resting cells.

An alternative measure of adhesion is the work done by the cantilever to detach the cell from immobilized ICAM-1. The work of de-adhesion includes work done to break the LFA-1–ICAM-1 complexes and to stretch the cell during this process. Work was derived by integrating the adhesive force over the distance traveled by the cantilever. Fig. 3 shows that

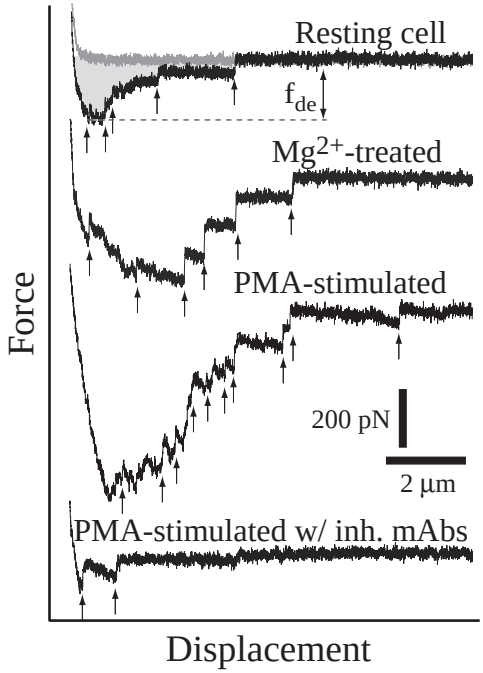

Fig. 2. Force versus displacement traces of the interaction between 3A9 cells and immobilized ICAM-1. The measurements were carried out with a resting cell (first trace), a Mg^{2+}-treated cell (second trace) and a PMA-stimulated cell (third trace). The measurements were acquired with a compression force of 200 pN, 5 seconds contact and a cantilever retraction speed of 2 μm/second. The fourth trace corresponds to a measurement acquired from a PMA-stimulated cell in the presence of LFA-1 (20 μg/ml FD441.8) and ICAM-1 (20 μg/ml BE29G1) function-blocking antibodies (inh. mAbs). The shaded area shows an estimate of the work of de-adhesion, and is the detachment force. Arrows point to breakage of LFA-1–ICAM-1 bond(s).

the enhancement in cell adhesion is more pronounced following cell activation when adhesion is expressed in terms of work of de-adhesion rather than in terms of detachment force. To demonstrate that the adhesion of both resting and activated cells is mediated by interactions of the LFA-1–ICAM-1 complex, we showed that cell adhesion is inhibited by antibodies against either LFA-1 or ICAM-1 and by 5 mM EDTA. Furthermore, 3A9 cells did not adhere to immobilized BSA. It should be emphasized that both the work of de-adhesion and the detachment force are functions of multiple parameters, including compression force, the contact duration and the retraction rate of the measurements. Hence, the comparison of the work of de-adhesion and the detachment force for different cases is valid for measurements carried out under identical conditions and should only be used to determine relative adhesion.

To determine if enhanced adhesion of PMA-stimulated cells is associated with an increase in receptor cooperativity (i.e. a simultaneous unbinding of two or more complexes), the magnitudes of the force transitions detected in the force-displacement traces were measured and plotted in the histograms presented in Fig. 4. Both resting and PMA-stimulated cells revealed a force distribution centered at ~ 45 pN. These force transitions are consistent with forces attributed to the unbinding of individual LFA-1–ICAM-1 complexes (Zhang et al., 2002). An observation that is more relevant to the current discussion is that the force distributions for resting and PMA-stimulated cells are nearly identical. On the basis of these measurements, there is no evidence for the simultaneous unbinding of multiple LFA-1–ICAM-1 complexes following PMA stimulation of the cells. If PMA did increase receptor cooperativity, then we would have detected a shift in the force distribution of the stimulated cells toward higher forces (Chen and Moy, 2000).

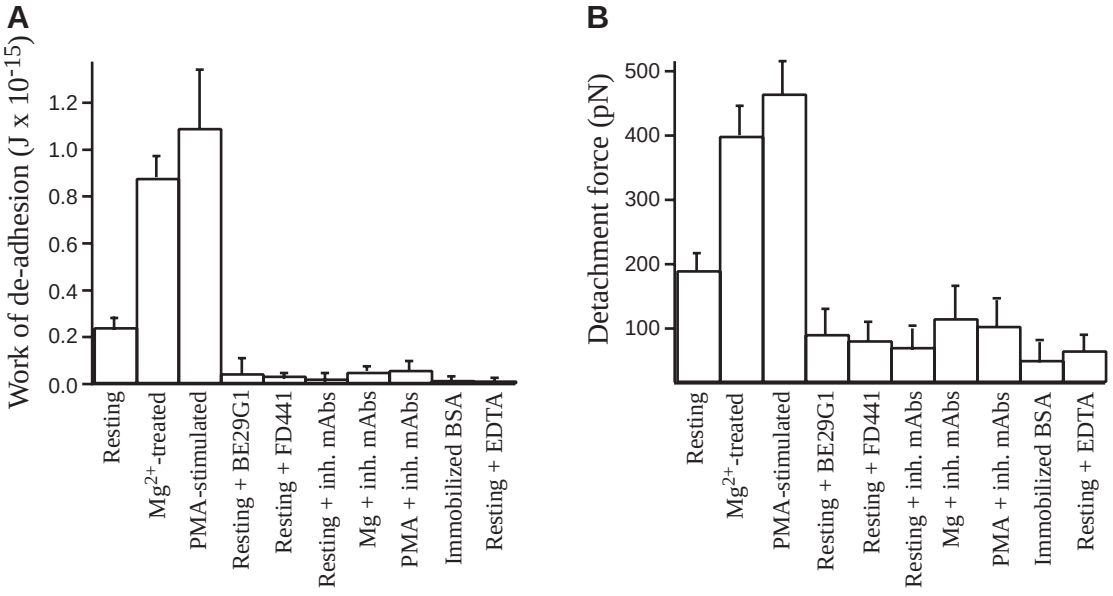

Fig. 3. Work of de-adhesion (A) and detachment forces (B) of resting and stimulated 3A9 cells bound to immobilized ICAM-1/Fc. The inhibitory monoclonal antibodies used were FD441.8 (anti-LFA-1; 20 μg/ml) and BE29G1 (anti-ICAM-1; 20 μg/ml). The numbers given here were derived from measurements that were acquired with a compression force of 200 pN, 5 seconds contact and a cantilever retraction speed of 2 μm/second. The error bar is the standard deviation and N>15 in each case (inh. mAbs, inhibitory antibodies).

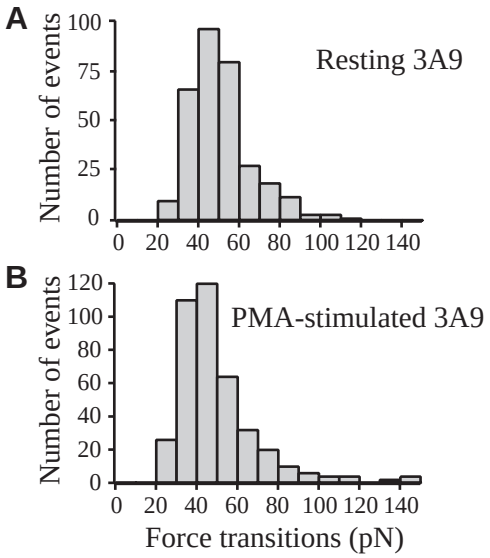

Fig. 4. Histograms of breakage forces of LFA-1–ICAM-1 bond(s) from the force-displacement traces of (A) resting and (B) PMA-stimulated 3A9 cells. The breakage forces were derived from the magnitude of the force transitions acquired in measurements obtained with a compression force of 200 pN, 5 seconds contact and a cantilever retraction speed of 2 μm/second. The y-axis plots the number of force transitions detected.

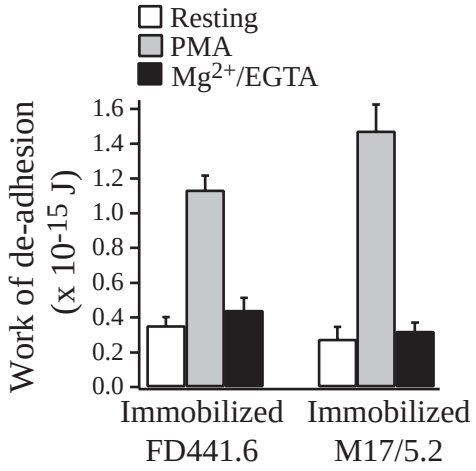

Fig. 5. Work of de-adhesion of resting (open bars), PMA-stimulated (gray bars), Mg^{2+}-treated (black bars) 3A9 cells bound to immobilized antibodies against LFA-1. The FD441.8 mAb recognizes an epitope formed by both α and β subunits of LFA-1. The M17/4.2 mAb recognizes an epitope on α_L. The numbers given here were derived from measurements that were acquired with a compression force of 200 pN, 2 seconds contact and a cantilever retraction speed of 2 μm/second. The error bar is the standard error.

In parallel experiments, we investigated the interactions between 3A9 cells and immobilized antibodies against LFA-1 (Fig. 5). The anti-LFA-1 monoclonal antibodies used in this study, M17/4.2 and FD441.8, recognized eptiopes on the α chain and the complexed αβ chains, respectively. Our force measurements revealed enhanced adhesion to immobilized M17/4.2 and immobilized FD441.8 for cells stimulated by PMA but not by Mg^{2+}. These results, along with the experiments described in the previous paragraphs, are consistent with observations made using more conventional cell adhesion assays (Stewart et al., 1996). Enhanced cell adhesion to immobilized ICAM-1 in response to Mg^{2+} can be attributed to an induced conformational change in LFA-1 that results in a high-affinity conformer of LFA-1. In contrast, the absence of enhanced adhesion to immobilized anti-LFA-1 suggested that the monoclonal antibodies bind to eptiopes that do not change following affinity modulation of LFA-1. However, enhanced cell adhesion to both ICAM-1 and anti-LFA-1 was detected in cells stimulated by PMA. These results revealed that enhanced adhesion to the antibodies following PMA is not the result of a conformational change in the ICAM-1-binding site of LFA-1.

Measurements of the unbinding forces of individual LFA-1–ICAM-1 complexes

To assess the bond strength of the individual LFA-1–ICAM-1 complexes, contact between the 3A9 cell and immobilized ICAM-1 was minimized by reducing both contact duration (~50 milliseconds) and compression force (~60 pN). Examples of measurements acquired under these conditions are given in Fig. 6A. In contrast to the measurements presented in Fig. 2, these measurements frequently revealed no adhesion. When adhesion did take place, the AFM force-displacement trace revealed a linear increase in force, followed by a single sharp transition that signaled the breakage of a single LFA-1–ICAM-1 complex. The unbinding force of the individual LFA-1–ICAM-1 complex was derived from the magnitude of the force transition with corrections for hydrodynamic drag. In order to determine the loading rate, the force spectra were plotted as force versus piezo displacement. We measured loading rates by multiplying the slope of the force versus displacement curve with the cantilever retraction speed. Fig. 6B summarizes the force distribution for the separation of the LFA-1–ICAM-1 complex at loading rates of 100 pN/second, 1000 pN/second and 30,000 pN/second. At a loading rate of 100 pN/second, the average force distribution was 30±2 pN (s.e.m.) for resting cells and became shifted to 64±1 when LFA-1 was activated by Mg^{2+}. Interestingly, the average force distribution did not change when the cells were stimulated by PMA (30±2 pN). At a loading rate of 1000 pN/s, the average force distribution was 54±2 pN (s.e.m.) for resting cells and was also shifted towards higher values averaging 100±3 pN for Mg^{2+}-activated LFA-1. Again, no change in the force distribution was detected when the cells were stimulated by PMA (51±2 pN). At 30,000 pN/s, histogram peaks had similar values in all three cases (240±6 pN for resting cells, 230±5 pN for PMA- stimulated cells and 240±7 pN for Mg^{2+}-activated cells).

As reported previously (Zhang et al., 2002), the average unbinding force of the LFA-1–ICAM-1 complex increases over three orders of magnitude change in loading rate (Fig. 7). Two loading regimes in the LFA-1–ICAM-1 interactions were evident in the force spectrum (plot of unbinding force versus loading rate). There was a gradual increase in unbinding force with an increasing loading rate up to about 10,000 pN/second.

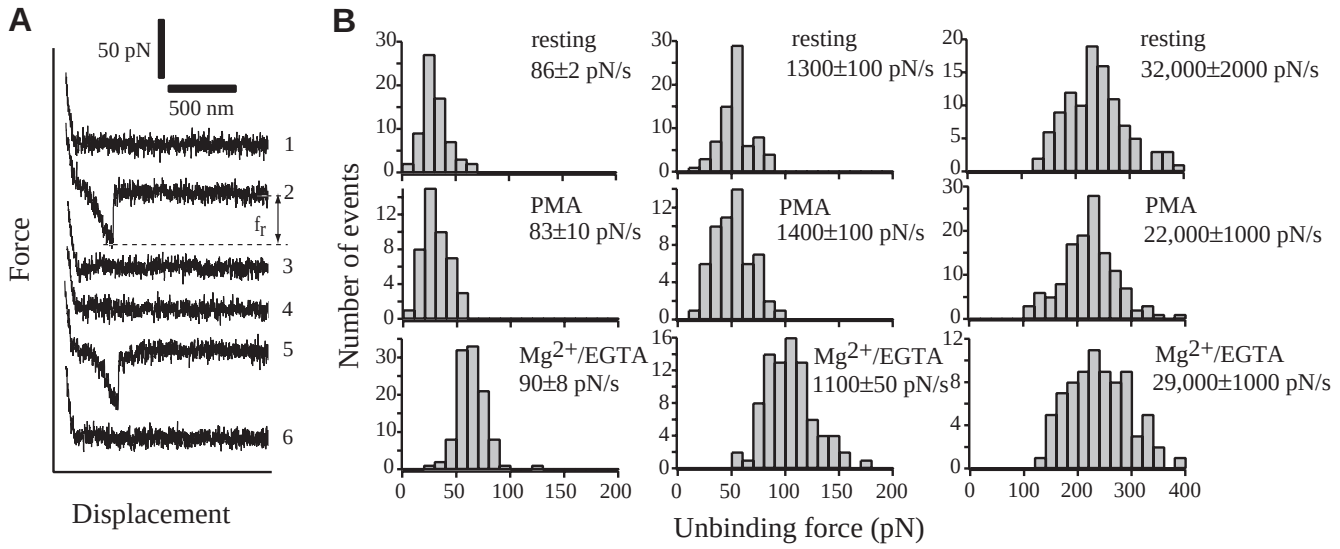

Fig. 6. (A) Measurements of unitary LFA-1–ICAM-1 unbinding forces. A series of AFM force measurements are shown. Traces 2 and 5 show molecular adhesion. Measurements of LFA-1–ICAM-1 unbinding forces were obtained under conditions that minimized contact between the 3A9 cell and the ICAM-1-coated surface. An adhesion frequency of less than 30% in the force measurements ensured that there is a >85% probability that the adhesion event is mediated by a single LFA-1–ICAM-1 complex (Tees et al., 2001). The specificity of the molecular interaction was confirmed by examining the frequency of adhesion in test and control experiments (Tees et al., 2001; Evans et al., 2001). Under identical experimental conditions, the addition of monoclonal antibodies against either LFA-1 or ICAM-1 significantly lowered the frequency of adhesion of both resting and activated cells. Moreover, both resting and stimulated 3A9 cells exhibited lower frequency of adhesion to immobilized bovine albumin than to immobilized ICAM-1. (B) Force histograms of unitary LFA-1–ICAM-1 unbinding forces of resting, PMA-stimulated and Mg^{2+}/EGTA-treated 3A9 cells at low (~73-98 pN/second) intermediate (~1050-1500 pN/second) and high (~21,000-35,000 pN/second) loading rates.

Beyond this point, there was a second loading regime that exhibited a faster increase in unbinding force. Induction of high-affinity LFA-1 by Mg^{2+}/EGTA resulted in higher LFA-1–ICAM-1 unbinding forces, which were pronounced in the slow loading regime. There was no significant difference in the dynamic response of the low- and high-affinity complexes in the fast loading regime (i.e. loading rates >10,000 pN/seconds). Cells that were activated with PMA, however, did not express a form of LFA-1 that exhibits a higher affinity for immobilized ICAM-1. As shown in Fig. 7, the force spectrum of the LFA-1–ICAM-1 complex acquired from PMA-stimulated 3A9 cells was superimposable on the measurements obtained from resting cells. Thus, measurements of the unbinding force of individual LFA-1–ICAM-1 complexes revealed that the observed enhanced cell adhesion following PMA stimulation (Figs 2 and 3) did not stem from a change in the intrinsic properties of the LFA-1–ICAM-1 interaction.

Elasticity of stimulated cells

Changes in elasticity of the cell may allow the cell to spread, leading to the formation of more adhesion complexes and, hence, greater adhesion. The mechanical properties of 3A9 cells were measured by AFM indentation measurements of cell elasticity. Fig. 8A presents typical force versus indentation curves obtained from resting and stimulated cells. The measurements were made with indentations of <1 μm and an indentation force of <1 nN in order to probe the cell without damaging it. (Forces >2 nN can damage the cell.) The fitted curves using the Hertz model were overlaid on the measurements. The average value for Young's modulus (N>300; 20-25 different cells) of the resting, Mg^{2+}/EGTA-treated and PMA-stimulated cells are 1.4±0.04 kPa, 3.0±0.09 kPa, and 0.30±0.01 kPa, respectively (Fig. 8C). Cells exposed to the equivalent amount of DMSO, used as a carrier in the PMA stimulation measurements, are unaffected. Thus, our measurements of cell elasticity revealed that the PMA-stimulated cells are softer than both resting and Mg^{2+}-treated cells. Fig. 8B includes histograms for resting, PMA-stimulated and Mg^{2+}-treated cells in order to show the data distribution for these experiments. The histogram for the resting cells revealed a peak around 0.6 kPa and another at around 1.5 kPa. The PMA-stimulated cell data histogram had a peak around 0.1 kPa and another around 0.35 kPa. This could indicate that the PMA caused a shift in the two populations of cells or that only some of the cells responded to PMA. The Mg^{2+}/EGTA-activated cells exhibited a broad data distribution.

Discussion

In this study, we used the AFM to elucidate the mechanisms of enhanced leukocyte adhesion following cell activation. Although both Mg^{2+} and PMA are capable of inducing enhanced adhesion in leukocytes, they achieve adhesion through different mechanisms. Extracellular Mg^{2+} binds directly to LFA-1, bypassing the requirement for inside-out signals to induce expression of high-affinity LFA-1. Recently, we showed by AFM that ICAM-1 complexed to the high-affinity form of LFA-1 was able to resist higher unbinding forces (Zhang et al., 2002). In contrast, the mechanisms by

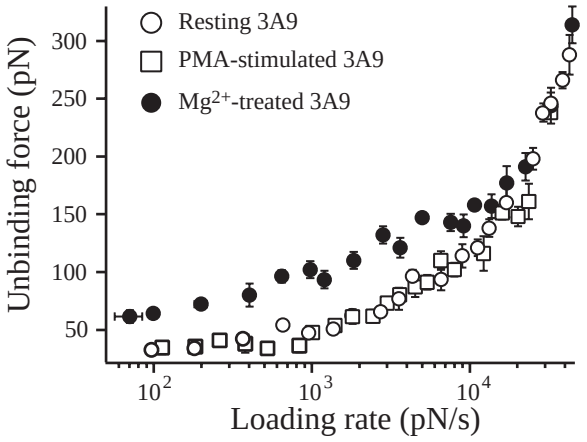

Fig. 7. Average unbinding force of individual LFA-1–ICAM-1 complexes as a function of force loading rate. Measurements were acquired using resting (open circle), PMA-stimulated (square) and Mg^{2+}/EGTA-activated (closed circle) 3A9 cells at loading rates between 20 and 50,000 pN/second. This range of loading rates was achieved by varying the retraction rate of the cantilever from 0.1 to 15 μm/second and as a result of variations in the local compliance of the cell. This allowed for the effective spring constant of the cell-cantilever combination to have a range of values between 0.1 and 5 mN/meter. At fast cantilever retraction speeds (>1 μm/second), the hydrodynamic drag on the cantilever resulted in smaller forces recorded than were actually applied to rupture the LFA-1–ICAM-1 complex (Evans et al., 2001). The damping coefficient of the cantilever ξ in the culture medium was ~2 pN-second/μm. Each of the force spectra were acquired using five cells with an average of 100 measurements/cell. The error bar is the standard error.

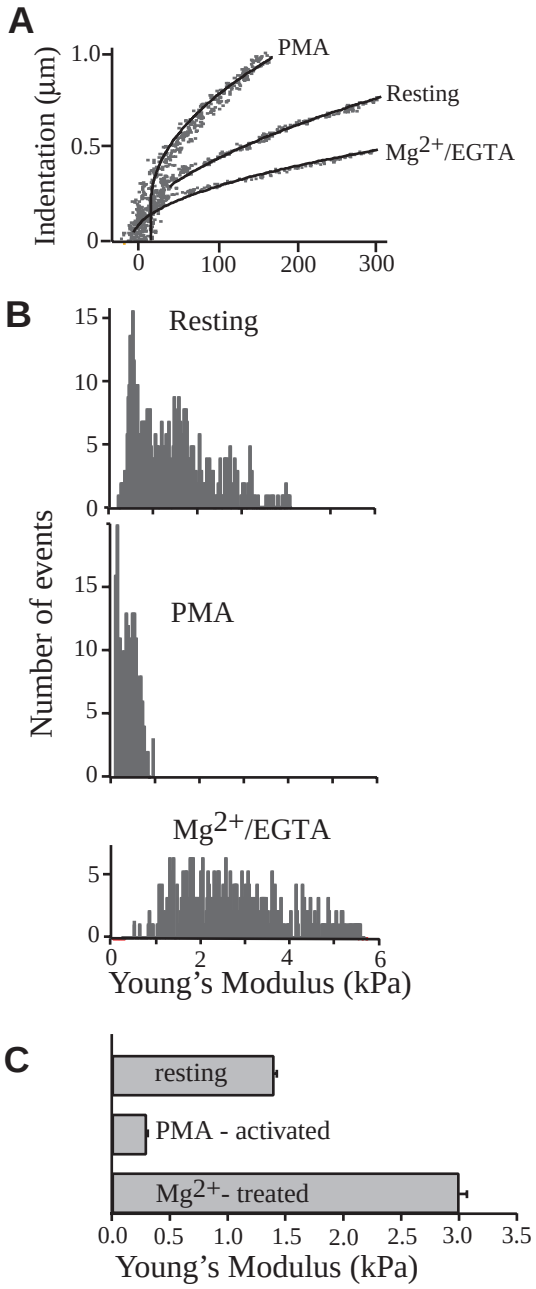

Fig. 8. (A) Force versus indentation traces of resting, PMA-stimulated and Mg^{2+}-treated 3A9 cells. The fitted curves derived from the Hertz model are overlaid on the measurements. (B) Histograms showing distribution of Young's modulus values for resting, PMA-stimulated and Mg^{2+}-treated 3A9 cells. (C) Young's modulus of resting, PMA-stimulated and Mg^{2+}-treated 3A9 cells. The error bar is the standard error.

which PMA contributes to leukocyte adhesion are less well defined. PMA exerts its effects through intracellular messengers, including cytoplasmic Ca^{2+}. Elevated Ca^{2+}, induced by PMA, activates calpain to release the cytoskeletal restraints of LFA-1 and promotes the clustering of mobile LFA-1. Here, we have demonstrated by using force measurements that the highly adhesive state of LFA-1 induced by PMA is not associated with changes in the bond strength of the individual LFA-1–ICAM-1 complex. This result is consistent with other studies that revealed that LFA-1 activation epitopes are not expressed in cells stimulated by PMA (Stewart et al., 1996). Instead, enhanced adhesion stemmed from an increase in the number of LFA-1–ICAM-1 complexes formed between the stimulated cell and the ICAM-1-coated surface.

LFA-1 polarization has been suggested as a mechanism for PMA-induced enhanced cell adhesion (Kupfer et al., 1990). However, it is unlikely that LFA-1 polarization is responsible for the enhanced adhesion observed in the time scale (~5 seconds) of AFM measurements following PMA-stimulation. A lateral redistribution of receptors is expected to change the local density of receptors, resulting in a higher receptor density in some areas and lower in others. If this were the case, we would have great irregularities in the AFM force measurements as areas of high and low receptor densities would contribute to high and low adhesion. We never detected a decrease in cell adhesion following PMA stimulation. The absence of a systematic decrease in cell adhesion suggested that the lateral redistribution of LFA-1 remained random and not directed toward or away from the area of cell contact. Since the average work of de-adhesion from many measurements was significantly higher for PMA-stimulated cells than for resting cells, we conclude that enhanced adhesion did not stem from a simple lateral redistribution of LFA-1.

It is conceivable that microclustering of LFA-1 can promote enhanced adhesion by distributing the applied force more evenly among the LFA-1–ICAM-1 complexes within the

microclusters. The formation of these clusters may lead to cooperativity among the LFA-1–ICAM-1 complexes during forced unbinding. However, our force measurements provided no evidence for cooperative unbinding of multiple LFA-1–ICAM-1 complexes. During the detachment of PMA-stimulated cells from immobilized ICAM-1, the majority of the rupture events (as indicated by a sharp transition in force, Fig. 6A) corresponded to the breakage of a single LFA-1–ICAM-1 complex (based on analysis of the magnitude of the force transitions). These results suggest that enhanced cell adhesion following PMA stimulation stemmed from an increase in the number of adhesion complexes formed between the cells and immobilized ICAM-1 rather than from the cooperative rupture of multiple adhesion complexes. It should be pointed out that a clustering of LFA-1 may still augment adhesion by distributing the applied force among the clustered LFA-1–ICAM-1 complexes even in the absence of cooperative unbinding of the LFA-1–ICAM-1 complexes.

In light of these observations, we explored other mechanisms by which cells can promote adhesion. Since there is good evidence that PMA promotes cell spreading, we postulated that PMA changes the elasticity of the cell, which, in turn, would allow the cell to deform and form greater contact with the apposing surface for a given applied force. Using the AFM, we measured the elasticity of resting, PMA-stimulated and Mg^{2+}-treated 3A9 cells. Our data did show that the PMA-stimulated cells were softer than both resting and Mg^{2+}-activated cells (Fig. 8C). The histograms for this elasticity data shown in Fig. 8B also revealed that there were two populations of resting and PMA-stimulated cells. We attribute this to two possible factors. One factor being the variability in membrane elasticity and the other changes in elasticity as a result of cell cycle changes. Our observations are consistent with a recent study by Matzke et al., who found using AFM in force mapping mode that fibroblast cells exhibit varied elasticities depending on their cell cycle stage (Matzke et al., 2001). Cells in interphase exhibited an elasticity of 1.0±0.4 kPa, cells in metaphase 1.7±0.9 kPa and cells at the onset of anaphase 3.0±2.5 kPa. The histogram for the Mg^{2+}-treated cells showed a broad data distribution with no major peak.

These AFM measurements of 3A9 cell elasticity revealed that the Young's modulus of the resting cell is ~1.4 kPa (Fig. 8C). An estimate of contact area A_c for a given compression force F, cell radius R and Young's modulus K is given by the Hertz model, that is,

$$A_c = \pi \times \sqrt[3]{\left(\frac{RF}{K}\right)^2}$$

(Israelachvili, 1992). For F=200 pN, R=5 μm and K=1400 Pa, the estimated contact area is ~2.5 μm^2. When K is reduced to 0.3 kPa following PMA-stimulation, the estimated area of contact is ~7.0 μm^2.

Assuming that the work of de-adhesion is proportional to the area of cell-substrate contact, changes in the elasticity of PMA-stimulated cells may give rise to a 280% increase in cell adhesion. It should be noted that another important component of the work of de-adhesion stems from the elastic deformation of the cell. An increase in cell compliance will increase the work of de-adhesion because softer cells are stretched more than stiffer cells during the detachment force of the LFA-1–ICAM-1 complexes. If the cell behaves like a linear system, the total work, W, done to deform the cell just before detachment is inversely proportional to k_c (i.e. $W=F^2/2k_c$). Hence, the measured ~fivefold increase in cell compliance following PMA activation is expected to result in a ~fivefold increase in the work of de-adhesion. However, this may be an overestimate (>20%) because a softer system will reduce the loading rate of the forced dissociation of the LFA-1–ICAM-1 complexes and hence lower the rupture force of the complexes.

In conclusion, the current study highlights the importance of cell compliance in leukocyte adhesion. Changes in the mechanical properties of the cell may result in an increase in the contact area, leading to greater adhesion. Moreover, increases in the compliance of the cell will increase the work required to induce separation of the LFA-1–ICAM-1 complexes. These changes in the mechanical properties of the cell can contribute to a >10-fold increase in the work of de-adhesion.

We thank C. Freites for technical support. This work was supported by grants from the American Cancer Society and the NIH (GM55611-01). X.Z. is supported by a predoctoral fellowship from the AHA.

References

Benoit, M. (2002). Cell adhesion measured by force spectroscopy on living cells. *Methods Cell Biol.* **68**, 91-114.

Benoit, M., Gabriel, D., Gerisch, G. and Gaub, H. E. (2000). Discrete interactions in cell adhesion measured by single-molecule force spectroscopy. *Nat. Cell Biol.* **2**, 313-317.

Berry, N. and Nishizuka, Y. (1990). Protein kinase C and T cell activation. *Eur. J. Biochem.* **189**, 205-214.

Chen, A. and Moy, V. T. (2000). Cross-linking of cell surface receptors enhances cooperativity of molecular adhesion. *Biophys. J.* **78**, 2814-2820.

Diamond, M. S. and Springer, T. A. (1994). The dynamic regulation of integrin adhessiveness. *Curr. Biol.* **4**, 506-517.

Dustin, M. L. and Springer, T. A. (1991). Role of lymphocyte adhesion receptors in transient interactions and cell locomotion. *Annu. Rev. Immunol.* **9**, 27-66.

Evans, E., Leung, A., Hammer, D. and Simon, S. (2001). Chemically distinct transition states govern rapid dissociation of single L-selectin bonds under force. *Proc. Natl. Acad. Sci. USA* **98**, 3784-3789.

Ganpule, G., Knorr, R., Miller, J. M., Carron, C. P. and Dustin, M. L. (1997). Low affinity of cell surface lymphocyte function-associated antigen-1 (LFA-1) generates selectivity for cell-cell interactions. *J. Immunol.* **159**, 2685-2692.

Grakoui, A., Bromley, S. K., Sumen, C., Davis, M. M., Shaw, A. S., Allen, P. M. and Dustin, M. L. (1999). The immunological synapse: a molecular machine controlling T cell activation. *Science* **285**, 221-227.

Heinz, W. F. and Hoh, J. H. (1999). Spatially resolved force spectroscopy of biological surfaces using the atomic force microscope. *Trends Biotechnol.* **17**, 143-150.

Hoh, J. H. and Schoenenberger, C. A. (1994). Surface morphology and mechanical properties of MDCK monolayers by atomic force microscopy. *J. Cell Sci.* **107**, 1105-1114.

Hughes, P. E., Diaz-Gonzalez, F., Leong, L., Wu, C., McDonald, J. A., Shattil, S. J. and Ginsberg, M. H. (1996). Breaking the integrin hinge. A defined structural constraint regulates integrin signaling. *J. Biol. Chem.* **271**, 6571-6574.

Huth, J. R., Olejniczak, E. T., Mendoza, R., Liang, H., Harris, E. A., Lupher, M. L., Jr, Wilson, A. E., Fesik, S. W. and Staunton, D. E. (2000). NMR and mutagenesis evidence for an I domain allosteric site that regulates lymphocyte function-associated antigen 1 ligand binding. *Proc. Natl. Acad. Sci. USA* **97**, 5231-5236.

Hutter, J. L. and Bechhoefer, J. (1993). Calibration of atomic-force microscope tips. *Rev. Sci. Instrum.* **64**, 1868-1873.

Hynes, R. O. (1992). Integrins: versatility, modulation, and signaling in cell adhesion. *Cell* **69**, 11-25.

Israelachvili, J. N. (1992). *Intermolecular and surface forces.* London: Academic Press.

Jones, S. L., Wang, J., Turck, C. W. and Brown, E. J. (1998). A role for the actin-bundling protein L-plastin in the regulation of leukocyte integrin function. *Proc. Natl. Acad. Sci. USA* **95**, 9331-9336.

Kolanus, W., Nagel, W., Schiller, B., Zeitlmann, L., Godar, S., Stockinger, H. and Seed, B. (1996). Alpha L beta 2 integrin/LFA-1 binding to ICAM-1 induced by cytohesin-1, a cytoplasmic regulatory molecule. *Cell* **86**, 233-242.

Kuhlman, P., Moy, V. T., Lollo, B. A. and Brian, A. A. (1991). The accessory function of murine intercellular adhesion molecule-1 in T lymphocyte activation. Contributions of adhesion and co-activation. *J. Immunol.* **146**, 1773-1782.

Kupfer, A., Burn, P. and Singer, S. J. (1990). The PMA-induced specific association of LFA-1 and talin in intact cloned T helper cells. *J. Mol. Cell Immunol.* **4**, 317-325.

Lollo, B. A., Chan, K. W., Hanson, E. M., Moy, V. T. and Brian, A. A. (1993). Direct evidence for two affinity states for lymphocyte function-associated antigen 1 on activated T cells. *J. Biol. Chem.* **268**, 21693-21700.

Lu, C., Shimaoka, M., Zang, Q., Takagi, J. and Springer, T. A. (2001). Locking in alternate conformations of the integrin alpha Lbeta 2 I domain with disulfide bonds reveals functional relationships among integrin domains. *Proc. Natl. Acad. Sci. USA* **98**, 2393-2398.

Lupher, M. L., Jr, Harris, E. A., Beals, C. R., Sui, L. M., Liddington, R. C. and Staunton, D. E. (2001). Cellular activation of leukocyte function-associated antigen-1 and its affinity are regulated at the I domain allosteric site. *J. Immunol.* **167**, 1431-1439.

Marlin, S. D. and Springer, T. A. (1987). Purified intercellular adhesion molecule-1 (ICAM-1) is a ligand for lymphocyte function-associated antigen 1 (LFA-1). *Cell* **51**, 813-819.

Matzke, R., Jacobson, K., Radmacher, M. (2001). Direct, high-resolution measurement of furrow stiffening during division of adherent cells. *Nat. Cell Biol*. **3**, 607-610.

Monks, C. R., Freiberg, B. A., Kupfer, H., Sciaky, N. and Kupfer, A. (1998). Three-dimensional segregation of supramolecular activation clusters in T cells. *Nature* **395**, 82-86.

Radmacher, M., Fritz, M., Kacher, C. M., Cleveland, J. P. and Hansma, P. K. (1996). Measuring the viscoelastic properties of human platelets with the atomic force microscope. *Biophys. J.* **70**, 556-567.

Rothlein, R. and Springer, T. A. (1986). The requirement for lymphocyte function-associated antigen 1 in homotypic leukocyte adhesion stimulated by phorbol ester. *J. Exp. Med.* **163**, 1132-1149.

Sanchez-Madrid, F., Simon, P., Thompson, S. and Springer, T. A. (1983). Mapping of antigenic and functional epitopes on the alpha- and beta-subunits of two related mouse glycoproteins involved in cell interactions, LFA-1 and Mac-1. *J. Exp. Med.* **158**, 586-602.

Shimaoka, M., Takagi, J. and Springer, T. A. (2002). Conformational regulation of integrin structure and function. *Annu. Rev. Biophys. Biomol. Struct.* **31**, 485-516.

Springer, T. A. (1990). Adhesion receptors of the immune system. *Nature* **346**, 425-434.

Stewart, M. and Hogg, N. (1996). Regulation of leukocyte integrin function: affinity vs. avidity. *J. Cell Biochem.* **61**, 554-561.

Stewart, M. P., Cabanas, C. and Hogg, N. (1996). T cell adhesion to intercellular adhesion molecule-1 (ICAM-1) is controlled by cell spreading and the activation of integrin LFA-1. *J. Immunol.* **156**, 1810-1817.

Stewart, M. P., McDowall, A. and Hogg, N. (1998). LFA-1-mediated adhesion is regulated by cytoskeletal restraint and by a Ca^{2+}-dependent protease, calpain. *J. Cell Biol.* **140**, 699-707.

Tees, D. F., Waugh, R. E. and Hammer, D. A. (2001). A microcantilever device to assess the effect of force on the lifetime of selectin-carbohydrate bonds. *Biophys. J.* **80**, 668-682.

van Kooyk, Y. and Figdor, C. G. (2000). Avidity regulation of integrins: the driving force in leukocyte adhesion. *Curr. Opin. Cell Biol.* **12**, 542-547.

Willemsen, O. H., Snel, M. M., Cambi, A., Greve, J., de Grooth, B. G. and Figdor, C. G. (2000). Biomolecular interactions measured by atomic force microscopy. *Biophys. J.* **79**, 3267-3281.

Woska, J. R., Jr, Morelock, M. M., Jeanfavre, D. D. and Bormann, B. J. (1996). Characterization of molecular interactions between intercellular adhesion molecule-1 and leukocyte function- associated antigen-1. *J. Immunol.* **156**, 4680-4685.

Wu, H. W., Kuhn, T. and Moy, V. T. (1998). Mechanical properties of L929 cells measured by atomic force microscopy: effects of anticytoskeletal drugs and membrane crosslinking. *Scanning* **20**, 389-397.

Zhang, X., Wojcikiewicz, E. and Moy, V. T. (2002). Force spectroscopy of the leukocyte function-associated antigen-1/intercellular adhesion molecule-1 interaction. *Biophys. J.* **83**, 2270-2279.

Zhou, X. and Li, J. (2000). Macrophage-enriched myristoylated alanine-rich C kinase substrate and its phosphorylation is required for the phorbol ester-stimulated diffusion of beta 2 integrin molecules. *J. Biol. Chem.* **275**, 20217-20222.